

LETTER TO THE EDITOR

Oxygen-defect-induced magnetism to 880 K in semiconducting anatase $\text{TiO}_{2-\delta}$ films

Soack Dae Yoon¹, Yajie Chen¹, Aria Yang¹, Trevor L Goodrich², Xu Zuo³, Dario A Arena⁴, Katherine Ziemer², Carmine Vittoria¹ and Vincent G Harris^{1,5}

¹ Center for Microwave Magnetic Materials and Integrated Circuits, Department of Electrical and Computer Engineering, Northeastern University, Boston, MA 02115, USA

² Department of Chemical Engineering, Northeastern University, Boston, MA 02115, USA

³ College of Information Technical Science, Nankai University, Tianjin 300071, People's Republic of China

⁴ National Synchrotron Light Source, Brookhaven National Laboratory, Upton, NY 11973, USA

Received 9 May 2006

Published 23 June 2006

Online at stacks.iop.org/JPhysCM/18/L355

Abstract

We demonstrate a semiconducting material, $\text{TiO}_{2-\delta}$, with ferromagnetism up to 880 K, without the introduction of magnetic ions. The magnetism in these films stems from the controlled introduction of anion defects from both the film–substrate interface as well as processing under an oxygen-deficient atmosphere. The room-temperature carriers are n-type with $n \sim 3 \times 10^{17} \text{ cm}^{-3}$. The density of spins is $\sim 10^{21} \text{ cm}^{-3}$. Magnetism scales with conductivity, suggesting that a double exchange interaction is active. This represents a new approach in the design and refinement of magnetic semiconductor materials for spintronics device applications.

(Some figures in this article are in colour only in the electronic version)

Recent research efforts on the growth of magnetically ordered semiconductor materials [1, 2] have received great attention because of potential new applications in spintronics devices [3]. The rationale for this optimism is the plausibility of integrating properties of both magnetic and semiconductor materials in new devices [1] (e.g. spin diodes [3–6] and spin-FETs [7]). Recent research has focused on dilute magnetic semiconductors (DMS) which were synthesized by introducing magnetic ions (e.g. Mn, Co, Fe, and etc) into conventional III–V [1, 2] and II–VI type semiconductors [8, 9] or wide bandgap semiconductors including ZnO and TiO_2 [8–13]. Also, ferromagnetism was induced in films of hafnium dioxide, HfO_2 , deposited by pulsed laser deposition (PLD) on sapphire substrates and attributed to defect doping [10–12]. Bulk HfO_2 is intrinsically non-magnetic and electrically insulating. This report has created intense

⁵ Author to whom any correspondence should be addressed.

debate as to the origins of magnetism in the Hf-dioxide film system [14–16]. In this letter, we have induced magnetism in films of $\text{TiO}_{2-\delta}$, which in its bulk form is non-magnetic and a wide bandgap semiconductor. It is also demonstrated that the amount of induced moment is systematically controlled by the oxidation pressure employed during PLD growth and by defects generated at the film–substrate interface.

Specifically, we chose a starting material of anatase $\text{TiO}_{2-\delta}$ and systematically introduced oxygen defects during the growth process. The TiO_2 material is known to be a wide bandgap semiconductor. Although stoichiometric TiO_2 contains only Ti^{4+} ions and is non-magnetic, unpaired 3d electrons in Ti^{3+} and Ti^{2+} ions can potentially cause magnetism. The formation of Ti^{3+} and Ti^{2+} requires the Ti ions to be stripped of electrons from the s band rather than the 3d band. This, for example, results in Ti^{3+} and Ti^{2+} ions having 3d¹ and 3d² electronic configurations, respectively. As is well known, oxygen vacancies create a charge imbalance and, therefore, a deviation from stoichiometric TiO_2 with the potential to generate Ti^{3+} and Ti^{2+} ions. The basic undertaking in this letter is to demonstrate the ability to control the concentration of oxygen defects and to explore their relationship to magnetism and transport in the oxide semiconductor. The anatase TiO_2 provides an interesting test bed for these studies, since in this structure the Ti cations form a 156° bond angle through the oxygen anion, which favours a superexchange interaction with high transition temperatures [17].

We have established for the first time a strong and unambiguous correlation between conductivity, induced magnetism, and oxygen pressure in $\text{TiO}_{2-\delta}$ films. Oxygen defects may originate from the processing of $\text{TiO}_{2-\delta}$ films in an oxygen-deficient atmosphere and at the interface between the anatase TiO_2 film and the rhombohedral structure of the (100) oriented lanthanum aluminate (LaAlO_3) [18] substrates. Films having the highest moments have magnetic transition temperatures near 880 K. Furthermore, we demonstrate a dependence of both conductivity and magnetization with sample thickness where thin films have the strongest magnetization, thus confirming the role of interfacial defects in inducing magnetism in these films.

Room-temperature stable rutile TiO_2 targets were prepared by conventional ceramic processing and used as ablation targets for PLD processing of anatase $\text{TiO}_{2-\delta}$ films on (100) LaAlO_3 substrates. The target was ablated using a KrF excimer laser ($\lambda = 248$ nm) with the substrate temperature fixed at 700 ± 1 °C (post-deposition cooling rate was ~ 10 °C min^{-1}). The laser output energy density focused on the target was 4 J cm^{-2} , and the oxygen pressure (p_{Ox}) was fixed during deposition at values ranging from 0.3 to 400 mTorr. A total of 6000 laser shots at a repetition rate of 1 Hz resulted in film thicknesses of ~ 200 – 300 nm.

The resulting $\text{TiO}_{2-\delta}$ films were measured by θ – 2θ x-ray diffraction (XRD) ($\text{Cu K}\alpha$ radiation). These data, depicted in figure 1, revealed only the (004) and (008) peaks consistent with the c -axis orientation of anatase crystals. The lattice mismatch between the anatase $\text{TiO}_{2-\delta}$ and the LaAlO_3 substrate was measured to be -0.26% . The c -axis lattice parameter, determined by peak profile fitting of (00 l) peaks, was 0.950 ± 0.0017 nm, which compares favourably with 0.952 Å for the bulk anatase structure of TiO_2 [19]. As seen in figure 1, there are clear distinctions between the position and amplitude of the anatase peaks and those of the rutile and substrate spectra. X-ray absorption spectroscopy in the region of the Ti $L_{2,3}$ absorption edge was performed at the National Synchrotron Light Source on beamline U4B and confirmed that the local structure symmetry of Ti was anatase.

Measured room-temperature conductivity of $\text{TiO}_{2-\delta}$ ranged from ~ 18 to ~ 0.03 $\Omega^{-1} \text{cm}^{-1}$ for films (film thickness ~ 300 nm) deposited at $p_{\text{Ox}} = 0.3$ and 10 mTorr, respectively. The $\text{TiO}_{2-\delta}$ films deposited at higher than 10 mTorr showed near-insulating behaviour at room temperature.

Figure 2 depicts the room-temperature magnetization of $\text{TiO}_{2-\delta}$ films as a function of the oxygen processing pressure from 0.3 to 400 mTorr (film thickness is ~ 270 nm). It is clear

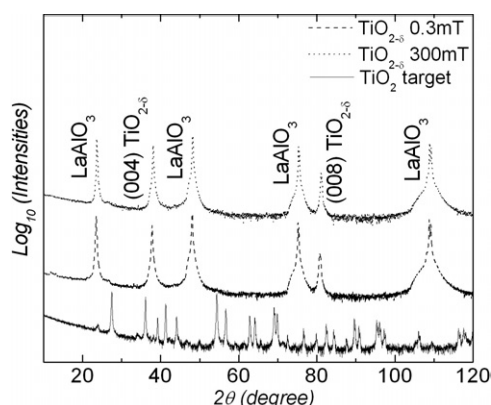


Figure 1. X-ray diffraction spectra of $\text{TiO}_{2-\delta}$ films and target material. Dashed and dotted curves correspond to data from films deposited at 0.3 and 300 mTorr, respectively. Similar data are provided for the rutile TiO_2 target material (solid).

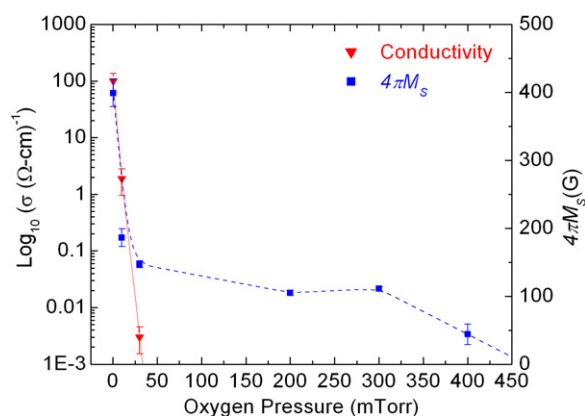


Figure 2. Room-temperature saturation magnetization ($4\pi M_s$) and conductivity as a function of oxygen processing pressure.

from these data that a strong relationship exists between magnetization and oxygen pressure, that is, the magnetization increases rapidly for low oxygen pressures. This suggests that the number of anion defects, or, conversely, the density of Ti^{3+} and Ti^{2+} cations, increases with a reduction in oxygen processing pressure. In addition, if anion defects are generating n-type carriers, one would expect the conductivity to increase. Such is the case, as we measure a logarithmic increase in the conductivity of films deposited at low pressures (see figure 2).

The static magnetic properties of the $\text{TiO}_{2-\delta}$ films at room temperature were measured using a vibrating sample magnetometer with the magnetic field applied parallel to the film plane. Samples showing magnetization were reproduced by multiple depositions under the same conditions. In the case of $p_{\text{O}_2} = 0.3$ mTorr, the sample having the highest magnetization, a total of five samples were deposited under identical conditions. The saturation magnetization (as $4\pi M_s$) of these samples was measured to be 420 ± 60 G, the coercive field was 150 ± 30 Oe, and the remanent magnetization was equal to 67 ± 7 G.

The magnetic moment as a function of temperature was measured from 77 to 750 K on a film deposited at a p_{O_2} of 0.3 mTorr. The film was magnetically saturated with an in-plane

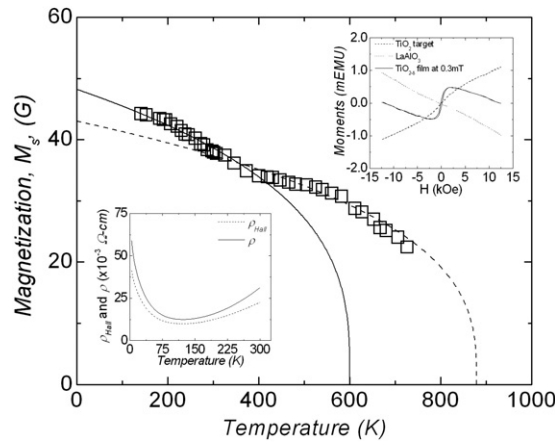


Figure 3. The temperature dependence of the magnetization for the $\text{TiO}_{2-\delta}$ film deposited at 0.3 mTorr of oxygen pressure. Room-temperature hysteresis loops (unprocessed) corresponding to the 0.3 mTorr processed film, a similarly prepared substrate (sans film), and the target material are presented as the upper right inset plot. DC resistivity and DC Hall resistivity versus temperature are presented as the lower left inset plot.

applied field of 2 kOe. Moment versus temperature data are shown in figure 3. We have applied the mean-field [20] approximation, $4\pi M_s \sim A4\pi N\mu(1 - \frac{T}{T_c})^\beta$, to fit the temperature-dependent saturation magnetization (figure 3), where N is the electron spin density, μ is the Bohr magneton, and A is an arbitrary constant. Figure 3 shows a second transition at a lower temperature, as is evidenced by the kink appearing around 450 K. Because of this, the data were fitted to two functions: one above and one below 400 K. The critical exponent (β) is predicted by mean-field theory to be ~ 0.5 [20]. In this manner, we determined a magnetic ordering temperature of 880 K (and a second transition temperature of ~ 600 K).

Ferromagnetic resonance (FMR) was measured on the $\text{TiO}_{2-\delta}$ films using a TE_{102} cavity at X-band frequency (9.5 GHz). One resonance was observed ($g \sim 2$) having a linewidth at 9.5 GHz of ~ 2 to 3 kOe, which is a value that is consistent with a defective $\text{TiO}_{2-\delta}$ structure.

AES (Auger electron spectroscopy) and XPS (x-ray photoelectron spectroscopy) showed impurity levels of Fe, Ni, and Co to be less than the detection threshold of these techniques, typically 0.1%, at the surface, throughout the film and at the substrate interface. This level of impurity concentration cannot account for the measured magnetic properties. We next address the role of defects in these films.

If one assumes that each oxygen defect results in a vacancy, in order to balance the charge around the defect, either one Ti ion must change its valence state from 4+ to 2+ or two Ti ions must change to 3+. Clearly, the Ti^{3+} or Ti^{2+} can potentially give rise to magnetism, since they represent $3d^1$ and $3d^2$ electronic configurations, respectively. The detection of magnetic Ti cations in TiO_2 samples is not without precedent. In an early paper, Senftle *et al* [21] attributed an enhanced magnetic susceptibility in bulk anatase TiO_2 to the presence of trivalent Ti cations. If the density of these defects is low, such that each Ti^{2+} or Ti^{3+} sites are isolated, then one would expect paramagnetism to result. In fact, targets of TiO_2 , likely to include significant defect concentrations, exhibit paramagnetism at room temperature. In our films, it is likely that the defects exist in localized regions of the film, i.e. as clusters or near the film/substrate interface. In these regions, superexchange interactions having a negative exchange will result in ferrimagnetism or antiferromagnetism. Alternatively, a positive exchange will result in ferromagnetism, i.e. via double exchange. If the defects are confined to the interfacial region,

one can envision that a percolation threshold can be overcome, thus giving rise to a carrier-mediated magnetism.

The number of net spins which give rise to the measured magnetization (at 0 K) can be approximated from $M(0) \approx Ng\mu S$, where N is the number of net spins between the superexchange sites, S is the spin at $T = 0$ K assuming that the orbital contribution is negligible, g is the splitting factor, and $\mu = 9.27 \times 10^{-21}$ ergs Oe $^{-1}$. This is also an approximate measure of the number of defects or the number of superexchange interactions occurring in the film. Taking $S = 1/2$ and $g = 2$, we estimate $N \sim 4 \times 10^{21}$ spins cm $^{-3}$. This corresponds to $\sim 0.15 \mu_B$ per Ti ion or one unpaired spin for every seven to eight Ti sites. X-ray magnetic circular dichroism (XMCD) was performed on the Ti L edge on beamline U4B at the National Synchrotron Light Source. These measurements did not reveal a ferromagnetic signal on the Ti edge. The absence of a ferromagnetic signal can be attributed to the low fraction of magnetic cations and their low moment. Also, XMCD was measured in total electron yield (TEY) mode, which is somewhat surface sensitive (probe depth ~ 4 – 10 nm). If ferromagnetic Ti cations are distributed away from the surface, perhaps clustered near the film/substrate interface, then XMCD in TEY mode would not detect their presence.

X-ray photoelectron spectroscopy was performed (using a PHI 04-173-0-077 Mg/Al dual-anode x-ray source with a PHI 10-360-4-015 hemispherical analyser) to investigate chemical bonding structure. As mentioned previously, neither XPS nor AES (performed using a PHI 15-110A CMA with 2 kV electron beam) showed any presence of Fe, Ni, or Co. Tight scan XPS analysis showed only one bonding state, likely Ti $^{4+}$ based on position, on the surface of the film. During destructive Ar $^{+}$ depth profiling, tight scan results indicate the presence of both Ti $^{2+}$ and Ti $^{3+}$ valence states throughout the film and at the interface. However, previous reports indicate that the Ar $^{+}$ sputter beam can give rise to these effects [18] and therefore these measurements are not definitive. A single bonding state at the surface of the TiO $_{2-\delta}$ film is to be expected, based on air oxidation after removal from the PLD chamber, and does not preclude the role of defects in the magnetization, as magnetic defect clusters are likely near the film/substrate interface.

The curve of measured magnetization versus temperature in figure 3 reveals two magnetic transitions: one near 600 K and the other at 880 K. We postulate that the lower-temperature transition corresponds to the T_C of the ferromagnetic exchange (Ti cations exchange coupled through oxygen), while the higher-temperature transition is the Néel transition of those sites that are ferrimagnetically coupled. This supposition stems from preliminary first-principles band structure calculations that will be presented in a future report. As is well known from studies of the double exchange interaction in magnetic oxides, [22, 23] ferromagnetism is energetically plausible in slightly conducting oxide systems such as this one. Usually, ferrimagnetism predominates in oxide magnetic systems (e.g. ferrites and garnets). Future studies are needed to clarify the underlying mechanisms in this film system.

As an inset to figure 3, room-temperature unprocessed hysteresis loops are presented for the 0.3 mTorr processed film, a similarly processed substrate (sans film), and the target material. It is noteworthy that the target and substrate samples were ~ 5000 times the volume of the film. It is clear from this plot that the substrate is diamagnetic, while the target is paramagnetic, and the film is either ferrimagnetic or ferromagnetic with a coercivity of 150 Oe.

In addition to magnetic characterization measurements, we have performed transport measurements. The dc Hall effect data and dc resistivity are presented as the other figure 3 inset. This measurement, performed at temperatures from 4 to 300 K, shows the film to be an n-type semiconductor with a carrier density of $\sim 3 \times 10^{17}$ cm $^{-3}$ at room temperature. The bottom of the conduction band in anatase is 3d-like thus, if the vacancy level is close to the bottom of the conduction band, the system is an n-type semiconductor where the carriers are d electrons.

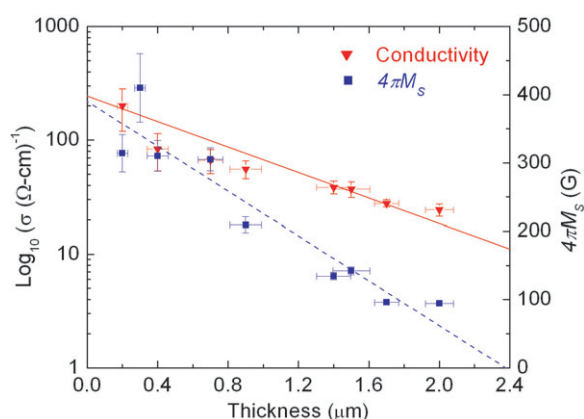


Figure 4. Room-temperature conductivity as a function of $\text{TiO}_{2-\delta}$ film thickness for samples grown at 0.3 mTorr oxygen pressure.

If interfacial defects contribute to the magnetism in the $\text{TiO}_{2-\delta}$ films, then one would expect that the effect would increase for thin samples and reduce for thicker films as the film relaxes to an unstrained state. Recently, the interfacial properties of anatase $\text{TiO}_{2-\delta}$ grown on rhombohedral (100) LaAlO_3 were reported [18]. In that report, it was found that the atomic mismatch at the $\text{TiO}_{2-\delta}$ film interface did indeed generate oxygen vacancies. In this mechanism, the defects provide a means to mediate the strain arising from the lattice mismatch at the interface. Due to these defects, the valences of the Ti ions change to maintain local charge balance. Hence, the transport properties of our defective films should reflect changes in defect concentration as well as the magnetization.

To explore the effects of interfacial defects on the magnetic properties of our films, a second series of films having thicknesses of 200 to 2000 nm was prepared under a fixed oxygen pressure of 0.3 mTorr. All other processing conditions were held the same. In figure 4, the log of conductivity is plotted on the same plot as the magnetization. There is a clear correspondence of increasing conductivity with increasing magnetization for decreasing film thickness. This is strong evidence that there exists interfacial oxygen defects in the $\text{TiO}_{2-\delta}$ films on (100) LaAlO_3 substrates that contribute to both transport and magnetism.

Next we address the possibility that magnetic contaminants are the source of the magnetism in these films. We considered two possible impurity conditions: the impurities may not have oxidized during deposition and exist as metallic clusters; or the impurities have oxidized where they exist as substitution, interstitial or cluster defects. AES and XPS measurements were performed to determine the level of magnetic impurities, namely Ni, Co, and Fe ions, present in these films. Measurements of our most magnetic films found impurity levels below 0.1%, which was the resolution threshold for these measurements. As a metallic impurity, only pure iron has sufficient magnetic moment to account for the measured magnetization. Since the saturation magnetization of metallic iron is about 20 kG at room temperature, a 0.1% Fe impurity level would provide a magnetization of 200 G at room temperature. However, FMR measurements revealed no traces of metallic Fe, even though as many as $\sim 10^{17}$ Fe spins would be present at that level of impurity. This is an amount that is easily detected by FMR. Secondly, through depth profiling, XPS measurements revealed no traces of Fe, Co, or Ni, oxidized or otherwise, in the films or at the interface.

It is also worth noting that the films were deposited at temperatures above 700 °C in an oxygen atmosphere, and it would be expected that Fe would have oxidized. Isolated impurities

of oxides of FeO, Fe₂O₃, NiO, and CoO would not contribute significantly to the measured moment, since their moments are much smaller than pure metallic Fe. However, one can imagine a situation where these ions occupy Ti sites with localized anatase coordination. These types of oxide clusters could contribute to, but not account for, the measured magnetization of the films. Again, XPS and AES revealed no measurable presence of these impurities at the surface, throughout the film, or at the interface. EPR (electron paramagnetic resonance) measurements on substrates revealed no features attributable to paramagnetic excitations of these oxides. We conclude that the levels of impurities are too low to account for the measured magnetic properties in these films. Finally, our films were handled exclusively using tungsten tweezers. In an earlier study, researchers found the handling of HfO₂ film samples with magnetic tweezers gave rise to measurable magnetism [14].

In conclusion, we have demonstrated a systematic technique whereby the semiconductor anatase TiO₂, when processed with anion defects, exhibits both magnetic and semiconducting properties at temperatures near 880 K. The room-temperature carriers are n-type with $n \sim 3 \times 10^{17} \text{ cm}^{-3}$. The density of spins is $\sim 10^{21} \text{ cm}^{-3}$. No evidence of magnetic impurities can be found that would explain the magnetic properties. The defects were introduced via the substrate lattice mismatch and by processing in an oxygen-deficient atmosphere. Magnetism scales with conductivity, suggesting that a double exchange interaction is active. This represents a new approach in the design and refinement of magnetic semiconductor materials for spintronics device applications above room temperature.

This research was supported, in part, by the US Office of Naval Research and the US National Science Foundation.

References

- [1] Ohno H 1998 *Science* **281** 951
- [2] Macdonald A H, Schiffer P and Samarth N 2005 *Nat. Mater.* **4** 195
- [3] Prinz G 1998 *Science* **282** 1660
- [4] Fiederling R *et al* 1999 *Nature* **402** 787
- [5] Ohno Y *et al* 1999 *Nature* **402** 790
- [6] Jonker B T *et al* 2000 *Phys. Rev. B* **62** 8180
- [7] Datta S and Daset B 1990 *Appl. Phys. Lett.* **56** 665
- [8] Matsumoto Y *et al* 2001 *Science* **291** 854
- [9] Fukumura T *et al* 2001 *Appl. Phys. Lett.* **78** 958
- [10] Venkatesan M, Fitzgerald C B and Coey J M D 2004 *Nature* **430** 630
- [11] Coey J M D *et al* 2005 *Phys. Rev. B* **72** 024450
- [12] Coey J M D 2005 *J. Appl. Phys.* **97** 10D313
- [13] Yoon S D *et al* 2006 *J. Appl. Phys.* **99** 08M109
- [14] Abraham D W, Frank M M and Guha S 2005 *Appl. Phys. Lett.* **87** 252502
- [15] Wang W *et al* 2006 *J. Appl. Phys.* **99** 08M117
- [16] Ramachandra Rao M S *et al* 2006 *Appl. Phys. Lett.* **88** 142505
- [17] Anderson P W 1956 *Phys. Rev.* **102** 1008
- [18] Sasahara A *et al* 2005 *Nanotechnology* **16** S18
- [19] Howard C J, Sabine T M and Dickson F 1991 *Acta Crystallogr. B* **47** 462
- [20] Kadanoff L P *et al* 1967 *Rev. Mod. Phys.* **39** 395
- [21] Senftle F E, Pankey T and Grant F A 1960 *Phys. Rev.* **120** 820
- [22] Zener C 1951 *Phys. Rev.* **82** 403
- [23] De Gennes P-G 1960 *Phys. Rev.* **118** 141